Multiaxial fatigue assessment of welded joints using the notch stress approach

Pedersen, Mikkel Melters

Multiaxial fatigue assessment of welded joints using the notch stress approach

M.M. Pedersen

Aalborg University, Department of Energy Technology, Pontoppidanstraede 101, DK-9220 Aalborg East, Denmark
(e-mail: mmp@et.aau.dk).

Abstract

This paper presents an evaluation of the safety involved when performing fatigue assessment of multiaxially loaded welded joints. The notch stress approach according to the IIW is used together with 8 different multiaxial criteria, including equivalent stress-, interaction equation- and critical plane approaches. The investigation is carried out by testing the criteria on a large amount of fatigue test results collected from the literature (351 specimens total). Subsequently, the probability of achieving a non-conservative fatigue assessment is calculated in order to evaluate the different criteria quantitatively. Large variation in safety is observed, especially for non-proportional loading.

Keywords: Welded joints, multiaxial fatigue, notch stress approach.

1. Introduction

Multiaxial fatigue loading in welded joints generally refers to normal stresses σ_x perpendicular to the weld interacting with shear stresses τ_{xy} parallel to the weld.

Two types of loading are considered; proportional (in-phase) loading and non-proportional (out-of phase) loading. For proportional loading, the principal stress directions remain constant and the situation is not that different from uniaxial loading of the weld at an angle. In the case of non-proportional loading, the principal stress directions may change over time which apparently causes the existing assessment procedures to fail.

The literature provides an abundance of criteria for assessment of welded joints under multiaxial loads, typically based on either stress interaction equations or critical plane approaches. However, there do not appear to be much consensus, neither in codes nor in the scientific literature, as to which multiaxial fatigue criterion is the most accurate. The purpose of this work is therefore to perform a rigorous evaluation of commonly applied multiaxial fatigue criteria.

In principle this evaluation could be based on either nominal-, structural- or notch stresses, or some of the more advanced quantities used for fatigue assessment e.g. based on strain energy density. Here, the notch stress approach according to the IIW is applied, in the hope that it will allow for the most unbiased comparison of test results obtained from specimens of different geometries, i.e. by limiting effects of differences in stress concentration.

We consider only welded steel joints, in as-welded condition, subjected to constant amplitude multiaxial loading transverse to the direction of the weld (excluding tests under longitudinal loading, because this case is not suited for assessment using the notch stress approach). A total of 351 fatigue test results could be found, which complied to these requirements, roughly half of these were tested under combined loading and the other half under pure uniaxial/shear loading.

This paper is organized in the following main parts: 2) review of multiaxial fatigue criteria for welded joints, 3) review of fatigue test data available in the open literature, and 4) evaluation of the multiaxial fatigue criteria against the experimental data.

2. Multiaxial fatigue criteria

The assessment criteria for multiaxial fatigue loading can be based on three concepts; equivalent stresses, interaction equations and critical plane approaches.

2.1. Equivalent stress and interaction equations

Early design codes typically specified an equivalent stress range in the form of either the von Mises or principal stress to be evaluated against the uniaxial SN curves [1]. More recent codes specify the use of interaction equations, in which the normal and shear stress components are evaluated individually against the corresponding uniaxial SN curve (e.g. EC3 or IIW).

Most criteria are generally not specific to any stress system, but are equally applicable using nominal/structural/ notch stresses. However, in the case of the notch stress approach, the IIW gives specific guidance [2], regarding the use of principal- and von Mises stresses. Both are limited to proportional loading, but here we test them also under non-proportional loading to illustrate the potential problems.

2.1.1. Principal stress

The maximum principal stress range is recommended for proportional loading when the minimum and maximum principal stress have the same sign and the influence of shear is less significant [2]. The range is calculated from the numerically largest of the maximum/minimum principal stress during the load cycle.

$$\sigma_1 = \left(\sigma_x + \sigma_y + \sqrt{(\sigma_x - \sigma_y)^2 + 4\tau_{xy}^2}\right)/2 \qquad (1)$$

Bäckström [3] investigated the use of the principal stress range as a damage parameter with the hot-spot stress approach but found a quite poor correlation, i.e. a scatter of almost an order of magnitude on the stress range.

Figure 1 shows why the principal stress approach fails for non-proportional loading. The calculated stress range is smaller for this case (b), when compared to proportional loading (a), which indicates that it would be less damaging. However, experiments, e.g. Siljander [4], show that the opposite is generally the case, i.e. that non-proportional loading is more damaging than proportional loading.

2.1.2. von Mises

The IIW recommends using the von Mises equivalent stress together with the notch stress approach in case of proportional loading and significant shear [2]. The von Mises equivalent stress range is calculated from the range of notch stress components

$$\Delta\sigma_{vM} = \sqrt{\Delta\sigma_x^2 + \Delta\sigma_y^2 - \Delta\sigma_x\Delta\sigma_y + 3\Delta\tau_{xy}^2} \qquad (2)$$

Another approach would be to calculate the von Mises stress over time and resolving the range from here. In such case, however, any (partial) compressive stress state would not contribute to the range, due to the strictly positive nature of the von Mises stress. The IIW approach (eq. 2) is therefore preferable.

One drawback of this approach is that it does not include any directional information; hence the most unfavorable direction of stress relative to the weld must be assumed in the analysis.

Sonsino [5] have showed this approach to be potentially non-conservative by up to a factor of 15 on life for non-proportional loading.
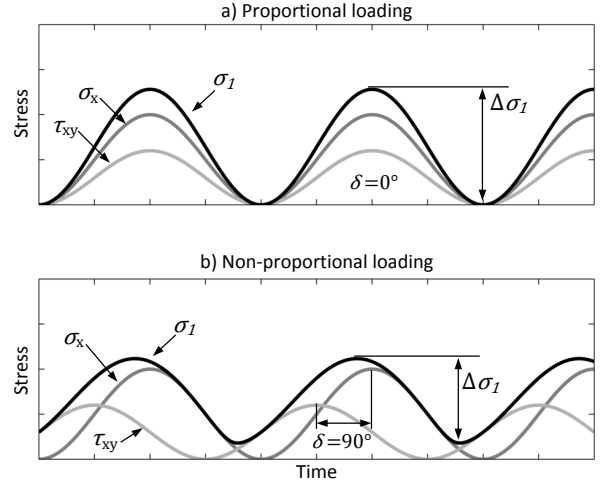

Figure 1: The range of principal stress is smaller for non-proportional loading than for proportional, after [1].

The IIW recommends using FAT200/3 together with the von Mises equivalent stress range [2]. Here, we evaluate all criteria against the same SN curve (FAT225/3) for comparison though. The FATxxx/y notation refers to an SN curve with fatigue strength *xxx* [MPa] at $N = 2 \cdot 10^6$ cycles and a slope of $m = y$.

2.1.3. Eurocode 3 approach

According to Eurocode 3 [6] welds subjected to multiaxial loading must be assessed using

$$\left(\frac{\Delta\sigma_x}{\Delta\sigma_R}\right)^3 + \left(\frac{\Delta\tau_{xy}}{\Delta\tau_R}\right)^5 \leq D_{EC3} \qquad (3)$$

Where $\Delta\sigma_R$ and $\Delta\tau_R$ are the uniaxial normal and shear fatigue strengths, respectively. The allowable damage sum is $D_{EC3} = 1.0$ for all cases. This is equivalent to the simple addition of the damage resulting from normal and shear stress, calculated independently of each other

$$D_\sigma + D_\tau \leq D_{EC3} \qquad (4)$$

No distinction between proportional and non-proportional loading is this made in this context. Eq.

(3) can be re-written to express a fatigue effective stress range

$$\Delta\sigma_{EC3} = \sqrt[3]{\Delta\sigma_x^3 + k \cdot \Delta\tau_x^5} \qquad (5)$$

where $k = \Delta\sigma_R^3/\Delta\tau_R^5$. This effective stress can then be evaluated against the uniaxial SN curve given by $\Delta\sigma_R$.

2.1.4. IIW approach

According to the IIW recommendations [7] welds subjected to multiaxial fatigue loading should be assessed using the Gough-Pollard equation

$$\left(\frac{\Delta\sigma_x}{\Delta\sigma_R}\right)^2 + \left(\frac{\Delta\tau_{xy}}{\Delta\tau_R}\right)^2 \le CV \qquad (6)$$

Where CV is a comparison value that takes the value 1.0 for proportional loading and 0.5 for non-proportional. The concept resembles that of EC3, where the damage from the two stress components is summed, however, the contents of eq. (6) cannot really be considered as damage due to the exponent of 2.

Eq. (6) can also be rewritten to express a fatigue effective stress range

$$\Delta\sigma_{IIW} = \frac{1}{\sqrt{CV}} \sqrt{\Delta\sigma_x^2 + k \cdot \Delta\tau_{xy}^2} \qquad (7)$$

where $k = \Delta\sigma_R^2/\Delta\tau_R^2$. Further limitations are imposed in the case of variable amplitude loading, however, this is not within the scope of this study.

2.2. Critical plane approaches

In critical plane approaches a number of search planes intersecting the surface either orthogonally and/or at some inclination are searched for the maximum value of a damage parameter.

The plane that maximizes the damage parameter is called the critical plane. Each search plane is defined by its unit normal vector **n**, which is again defined by the angle to the local x-axis θ and the inclination angle ϕ as shown in Figure 2.

The stress tensor in each material point is needed as the starting point for the analysis, i.e.

$$\boldsymbol{\sigma} = \begin{bmatrix} \sigma_{xx} & \tau_{xy} & \tau_{xz} \\ \tau_{xy} & \sigma_{yy} & \tau_{yz} \\ \tau_{xz} & \tau_{yz} & \sigma_{zz} \end{bmatrix} \qquad (8)$$

The stress tensor is generally a function of time, but this is not shown due to clarity. The stress vector acting on a search plane can be calculated as

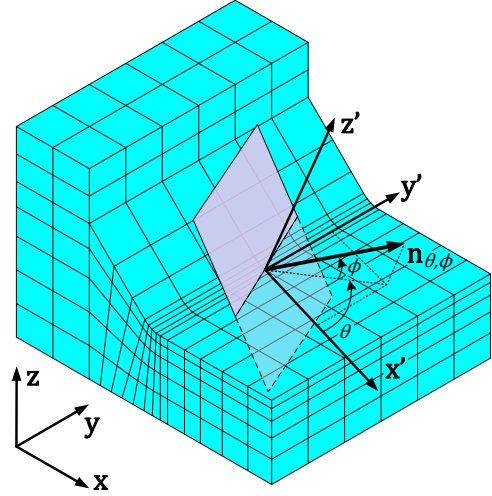$$\mathbf{S_n} = \boldsymbol{\sigma}\mathbf{n} \qquad (9)$$

Figure 2: Search plane in the notch radius. Note that the notch coordinate system is slightly inclined, such that the z'-axis is normal to the notch surface.

The stress vector can then be divided in a component normal to the plane, i.e. the normal stress

$$\sigma_{\mathbf{n}} = \mathbf{nn}^T \boldsymbol{\sigma}\mathbf{n} \qquad (10)$$

and parallel to the plane, i.e. the shear stress

$$\boldsymbol{\tau} = \mathbf{S_n} - \sigma_{\mathbf{n}} = \boldsymbol{\sigma}\mathbf{n} - \mathbf{nn}^T \boldsymbol{\sigma}\mathbf{n} \qquad (11)$$

For proportional loading, the shear stress vector $\boldsymbol{\tau}$ has a constant direction; however under non-proportional loading, it describes some trajectory in the search plane, whereas only the magnitude of the normal stress will change, see Figure 3. In the latter case, the extraction of shear stress range is not trivial, and a multitude of approaches have been proposed for this. Here, we use the Longest Chord method [8] which is sufficient for the relatively simple trajectories obtained from sinusoidal loading.

In this work the set of search planes is limited to $\theta = 0 - 180°$ and $\phi = 0 - 90°$ in 5° steps.

The critical plane approach was originally developed for multiaxial fatigue assessment of non-welded components, but several extensions have been proposed for welded joints, as will be explained in the following.

2.2.1. EESH by Sonsino

Sonsino [9] proposed a critical plane oriented integral hypothesis called Effective Equivalent Stress Hypothesis (EESH) for multiaxial fatigue assessment of ductile materials, e.g. welds in structural steel.
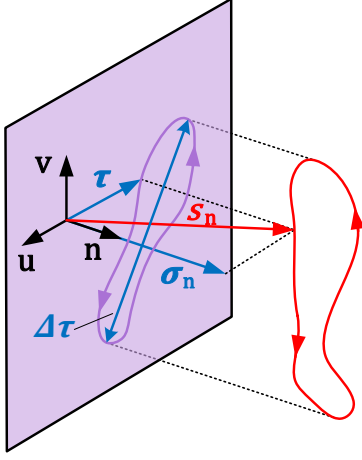
Figure 3: Example stress trajectory under non-proportional loading.

Here, the damage parameter F is calculated as an integral value of the shear stress over all search planes orthogonal to the surface ($\phi = 0°$). The reason behind the integral approach is that damage is assumed to accumulate on multiple planes under non-proportional loading.

$$F(\theta) = \frac{1}{\pi} \int_0^\pi \tau(\theta) d\theta \qquad (12)$$

The effective equivalent stress can then be calculated from this damage parameter, depending on the phase-shift of the loading δ

$$\Delta\sigma_{EESH}(\delta) = \Delta\sigma_{EESH}(0°) \frac{F(\delta)}{F(0°)} \sqrt{S^z} \qquad (13)$$

where

$$\Delta\sigma_{EESH}(0°) = \sqrt{\Delta\sigma_x^2 + \Delta\sigma_y^2 - \Delta\sigma_x\Delta\sigma_y + f_s^2 \cdot 3\Delta\tau_{xy}^2} \qquad (14)$$

and

$$f_s = \sqrt{\Delta\sigma_{Rx}^2 + \Delta\sigma_{Ry}^2 - \Delta\sigma_{Rx}\Delta\sigma_{Ry} + 3\Delta\tau_R^2} \qquad (15)$$

$$S = \frac{1 + K_{t,\sigma}}{1 + K_{t,\tau}} \qquad (16)$$

$$z = 1 - \left(\frac{\delta - 90°}{90°}\right)^2 \qquad (17)$$

The size factor f_s is calculated from the local fatigue strength and includes a transverse component calculated as $\Delta\sigma_{Ry} = \mu \cdot \Delta\sigma_{Rx}$. The effective equivalent stress (13) is then evaluated against the SN curve for uniaxial normal stress.

Sonsino and Lagoda [10] successfully applied the EESH together with an early version of the notch stress approach based on a fictitious radius of $1mm$.

2.2.2. Carpinteri and Spagnoli (C-S)

Carpinteri et al. [11] proposed a rather simple approach in which the critical plane orientation can be determined a priori. The orientation of the critical plane is assumed to coincide with the principal stress directions at the time instant where the first principal stress achieves its maximum during the load cycle.

The damage parameter is defined as a fatigue effective stress consisting of a non-linear combination of the normal and shear stress ranges occurring on the critical plane, modified by the squared ratio of normal to shear fatigue strength at fully reversed loading ($R = -1$).

$$\Delta\sigma_{C-S} = \sqrt{\Delta\sigma_{eq}^2 + k \cdot \Delta\tau^2} \qquad (18)$$

where $k = \Delta\sigma_{R,-1}^2 / \Delta\tau_{R,-1}^2$. The equivalent normal stress in (18) is defined by including the Goodman mean stress correction as follows

$$\Delta\sigma_{eq} = \Delta\sigma + \Delta\sigma_{R,-1} \frac{\sigma_m}{R_m} \qquad (19)$$

Here, a common value for tensile strength equal to $R_m = 520MPa$ is used. Apart from the mean stress correction eq. (18) corresponds to the Gough-Pollard equation as given in (6), but here it is applied in a critical plane manner.

The fatigue strength for fully reversed loading $\Delta\sigma_{R,-1}$ is generally not available in an engineering context, since codes and recommendations do not relate the fatigue strength of welded joints to the stress ratio (R). We thus apply the standard fatigue strength $\Delta\sigma_R$ here, as would be the logical solution in practice.

The criterion was tested by Carpinteri et al. [11] using SN curves derived from the experimental data in the nominal stress system. They found a fairly good and mostly conservative correlation between the predictions and experimental data.

2.2.3. Findley Criterion

The Findley criterion [12] is a shear stress based critical plane criterion which predicts failure on the plane that maximizes the damage parameter

$$f = \tau + k\sigma_{max} \qquad (20)$$

Here τ is the shear stress amplitude, σ_{max} is the maximum normal stress occurring over a load cycle. k is an experimentally determined material factor describing

the sensitivity to normal stress assumed to be $k = 0.3$ [13].

This criterion has been applied for welded joints in original or modified form e.g. [4], [3], [13] and [14].

In its original formulation, infinite life was predicted if the damage parameter is below some experimentally determined threshold value $f \leq f_{crit}$. Recently, Bruun and Härkegård [15] demonstrated how the Findley criterion may be reformulated in terms of an equivalent stress amplitude to be evaluated against the uniaxial fatigue resistance instead of f_{crit}, i.e.

$$\Delta\sigma_F = \frac{\Delta\tau + 2k\sigma_{max}}{\frac{1}{2}(k + \sqrt{1 + k^2})} \leq \Delta\sigma_R \qquad (21)$$

This is the formulation applied here. The implication of using this formulation compared to the original (and taking $f_{crit} = \Delta\sigma_R$) corresponds to a magnification factor of 1.49 on the stress range (for $k = 0.3$).

2.2.4. MWCM by Susmel

The Modified Wöhler Curve Method (MWCM) according to Susmel [16] is a shear stress based critical plane approach, i.e. the critical plane is assumed to be that attaining the largest shear stress range during the load cycle. The basic idea in this approach is to derive a load-specific SN curve suitable for the actual combination of normal and shear stress, see Figure 4.

The derivation is based on the stress ratio

$$\rho_w = \frac{\Delta\sigma_n}{\Delta\tau} \qquad (22)$$

On the critical plane (max shear stress plane), the stress ratio is 0 for pure torsion and 1 for pure bending/tension.

The modified SN curve is derived from two SN curves - one for normal stress ($\Delta\sigma_R$ and m_σ) and one for shear stress ($\Delta\tau_R$ and m_τ), obtained from code or experiments.

The slope is determined as

$$m_m(\rho_w) = (m_\sigma - m_\tau)\rho_w + m_\tau \qquad (23)$$

The slope is limited by that of the normal stress SN curve, i.e. $m_m \geq m_\sigma$. The modified shear stress resistance is then found from

$$\Delta\tau_{Rm} = \left(\frac{\Delta\sigma_R}{2} - \Delta\tau_R\right)\rho_w + \Delta\tau_R \qquad (24)$$

A limit of $\rho_w \leq \Delta\tau_R/(2\Delta\tau_R - \Delta\sigma_R)$ is enforced in order to avoid over-conservative results.
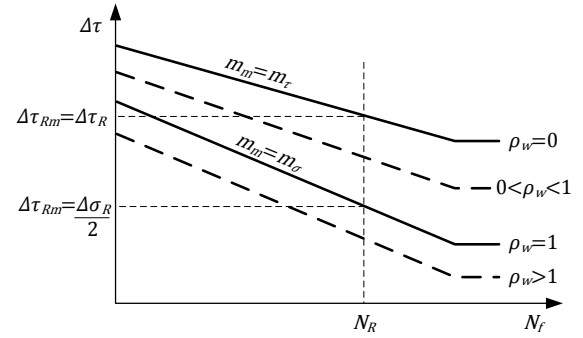

Figure 4: Modified SN curves, after [16]

The damage parameter in this criterion is the shear stress range on the critical plane which is evaluated against the modified SN curve.

Susmel [17] used the MWCM together with the notch stress approach and obtained good results when using the rotated SN curves ($m_\sigma = 5$ and $m_\tau = 7$) proposed by Sonsino [18] for "thin and flexible joints", although with a high level of conservatism in some cases.

3. Experimental investigations

Surprisingly few experimental investigations have been carried out on multiaxial fatigue in welded joints. Only the 12 investigations listed in Table 1 could be found which complied with the limitations of this study, i.e. steel base material, as-welded condition and constant amplitude loading.

Table 1: Experimental studies of welded joints under multiaxial loads, see also Table A.3.

Primary author	t [mm]	Loading Primary	Loading Secondary
Siljander [4]	9.5	Bending	Torsion
Bäckström [3]	5	Bending	Torsion
Yung [19]	8	Bending	Torsion
Sonsino TP [9]	10	Bending	Torsion
Sonsino TT [9]	6	Bending	Torsion
Witt [20]	8	Bending	Torsion
Amstutz [21]	10	Bending	Torsion
Yousefi [22]	8	Bending	Torsion
Razmjoo [23]	3.2	Tension	Torsion
Archer [24]	6	Bending	Shear
Dahle [25]	10	Bending	Torsion
Takahashi [26]	12	Tension	Tension

According to the IIW [2], the notch stress approach with $r_{ref} = 1mm$ should only be applied for $t \geq 5mm$,

thus including the tests of Razmjoo [23] and Dahle [3] is questionable. However, as will be seen later, these results agree well with the others and are therefore kept in the analysis.

The majority of the results from Dahle [25] are excluded since the specimens were cracking in a longitudinally loaded weld and thus are not suitable for assessment using the notch stress approach. Only the specimens cracking from the transverse butt weld (TW) are included. These results are corrected by a factor k_m = 1.10 for misalignment, according to IIW recommendations [7]. The results from Takahashi [26] are divided in two groups, because the specimens were slightly different in the uniaxial case (U) compared to that used for the biaxial case (L).
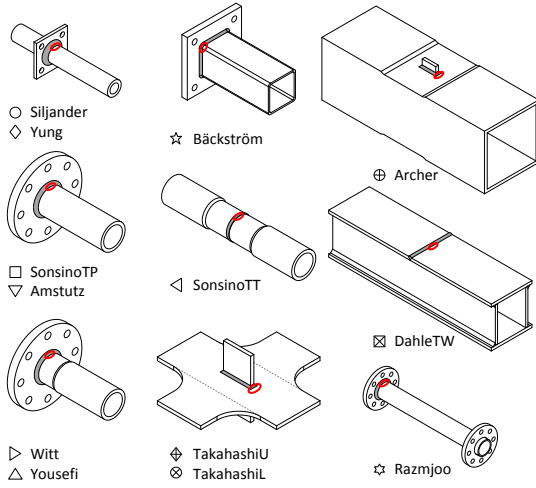

Figure 5: Fatigue test specimens (same scale).

3.1. Test conditions

The experimental work was carried out under different test conditions regarding geometry, loading, mean stress, residual stress (stress relieving) and weld quality. This will of course lead to more scatter in the results, but it will also allow for testing the multiaxial criteria under a wide variety of conditions.

3.2. Notch stress analysis

Detailed finite element analysis was carried out for all specimen geometries according to the IIW recommendations [2], i.e. using a reference radius of r_{ref} = 1mm and second order elements smaller than 0.25mm in the notch. Figure 6 shows an example FE model including a close-up of the typical mesh in the weld toe. For the cases where the weld leg length is not reported in the reference, it was set equal to the plate thickness.
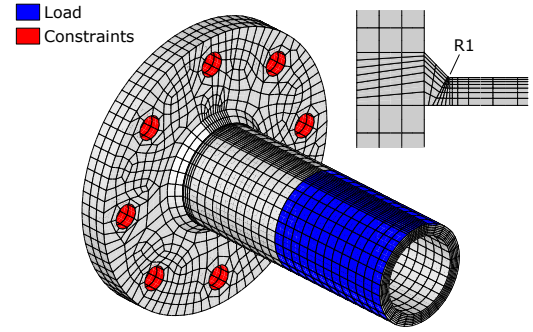

Figure 6: FE model example including close-up of notch mesh.

The FE models of the tube-to-plate specimens were constrained in the bolt holes, shown in Figure 5, and not on the back face of the plate. This led to almost identical stress levels as obtained in a non-linear FE model with bolts and friction (within 10%). Fixing the entire back face of the plate on the other hand led to greatly underestimated stress levels, e.g. a factor 2 difference to the non-linear model.

Unity nominal stress in bending/tension/torsion/shear was then applied to the models and the notch stress tensor could be determined, see Table A.4. The node displaying the maximum normal stress under the primary load was selected as the location of investigation. The reason behind this choice is that the normal stress exhibits a peak value somewhere on the geometry, whereas the shear stress due to torsion was generally more evenly distributed.

Typically, the selected node was located not on the edge of the radius, but some distance into the radius. Therefore a notch coordinate system was introduced at this location with the z-axis normal to the curved face of the notch, see Figure 2. The inclination of the notch coordinate system was typically 15° relative to horizontal.

Although minor, this inclination of the notch coordinate system makes a difference when setting up the search planes for calculating the notch stress in the critical plane approaches.

The notch stress tensor time histories of all specimens were then established from superposition of the values in Table A.4 multiplied with the nominal stress trajectories given in the references. The stress range could then be resolved from the notch stress history according to the different multiaxial criteria.
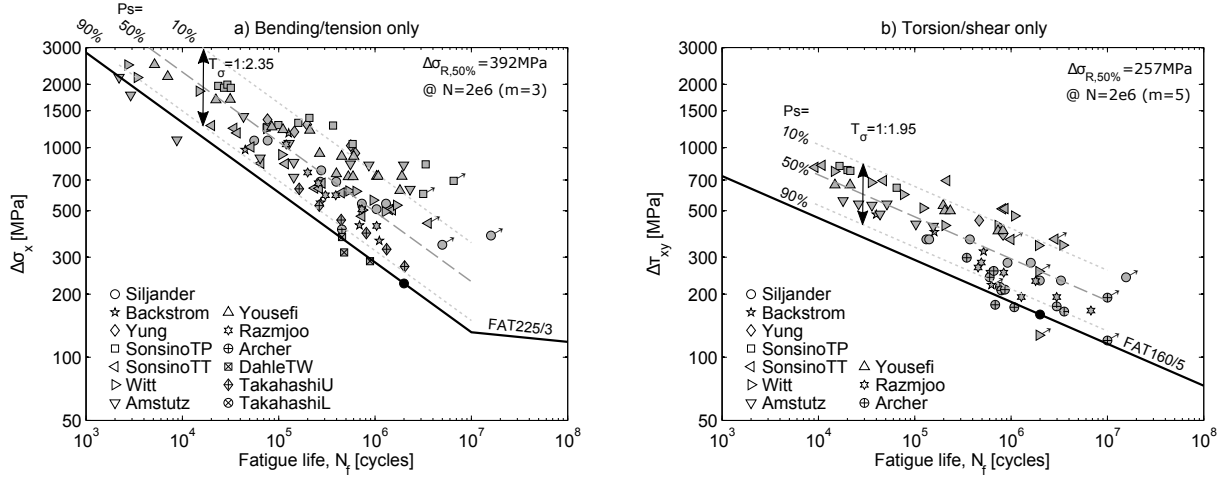
6

Figure 7: Compiled fatigue test results for bending/tension only test results (left) and torsion/shear only test results (right). Results shown in the notch stress system.

3.3. Reference SN curves

In order to apply any of the multiaxial criteria it is necessary to establish two reference uniaxial SN curves, i.e. for pure normal- and shear stress. Here, FAT225/3 and FAT160/5 are applied, as recommended by the IIW [7] and Sonsino [27].

The validity of these curves is briefly examined in the following by comparing them against the relevant uniaxial fatigue data. As seen in Figure 7(left) the normal stress SN curve FAT225/3 covers the data very well.

It should be kept in mind though, that several of the test results stems from specimens subjected to stress relieving, which usually improves the fatigue resistance. Yung and Lawrence [19] however found stress relieving to be detrimental, because the residual stress state at the critical location in the weld toe was compressive in their specimens.

Furthermore, the SN-curve provided by the IIW is derived for welds subjected to high tensile residual stresses. This condition is typically simulated by performing the fatigue test at a high stress ratio $R = 0.5$. The fatigue tests considered here were generally carried out under low stress ratios, i.e. $R = -1$ and $R = 0$, though.

It is thus clear that there is a discrepancy between the test results and the SN curve. However, due to the unknown residual stress state of the specimens and likewise uncertain effect of stress relieving, no corrections have been applied to account for this.

Another issue that adds to the scatter in the results is weld quality, in particular the weld toe radius. Unfortunately, this important value is typically not recorded and its influence on the results can thus not be quantified. Jonsson et al. [28] showed that the weld toe radius is highly influenced by the direction of gravity relative to the weld during welding. They found a difference of more than 60% on the fatigue strength of fillet welds welded in lying and standing position, respectively, and credited this difference to the influence of gravity in forming the weld toe radius. For the specimens considered in this investigation one could thus expect the same difference depending on whether the specimens were welded in lying or standing position.

Sonsino [27] proposed using FAT160/5 for the assessment of welded joints loaded in pure torsion/shear. As seen from Figure 7(right) this curve also fits the experimental data very well. It covers all the data, except 2 from Archers investigation.

Sonsino [18] also observed that in some cases, fatigue tests of thin/flexible specimens tend to give results following an SN curve with a shallower slope. He therefore suggested using slopes of $m_\sigma = 5$ and $m_\tau = 7$ for normal- and shear stress, respectively, in such cases. However, according to Figure 7, the usual slopes of $m_\sigma = 3$ and $m_\tau = 5$ seems to fit the data sufficiently well.

The result of an evaluation such as this one is of course highly dependent on the selected reference SN curves. Better results than presented here are often seen

in the literature e.g. based on experimentally determined mean SN curves. In this work, however, we use the standard/accepted design SN curves as provided by the IIW [2] and [27] in order to shed light on the safety of the assessments carried out in practical engineering.

4. Evaluation

In the following we evaluate the 8 multiaxial fatigue criteria by applying them to the collected fatigue test data for combined loading, omitting the uniaxial results for clarity.

All the fatigue test data are plotted in SN diagrams using the calculated equivalent uniaxial stress range for each criteria for comparison against the FAT225/3 SN curve. The markers are color-coded according to the loading (light for proportional and dark for non-proportional) and the marker shape indicates the author/specimen of the original investigation, see Figures 8 and 9.

The MWCM results cannot be directly plotted in the same form because this method uses differentiated SN curves depending on the specific loading conditions of each test specimen. Instead, we consider the experimentally determined life vs. the calculated life in Figure 9d.

In the typical statistical analysis of fatigue data for welded joints, all data points are recalculated to the same stress range in order to fit a log-normal distribution to the N-data and subsequently calculate the probability of failure relative to an SN curve. e.g. [7]. In case of the MWCM, this is not possible, since the method uses a modified SN curve for each data point, i.e. the population of test results do not refer to the same SN curve. This feature of the MWCM makes quantitative comparison of the criterion against other criteria difficult.

In order to overcome this difficulty, a prediction ratio similar to the one employed by Bruun and Härkegård [15] is introduced

$$p = \frac{\Delta\sigma_{eq,N,i}}{\Delta\sigma_{R,N}} \qquad (25)$$

Here, $\Delta\sigma_{eq,i,N}$ is the equivalent stress range at N cycles for the i'th specimen and $\Delta\sigma_{R,N}$ is the design fatigue strength at the same number of cycles. It thus describes the ratio of experimentally determined fatigue strength to the theoretical fatigue strength for each specimen. Therefore $p < 1$ indicates a non-conservative prediction and $p \geq 1$ means that the prediction is conservative, i.e. the data point at hand is at or above the SN curve.

The advantage of using this prediction ratio is that it can be applied equally well for criteria based on a equivalent (modified) stress range and to criteria relying on a modified fatigue strength, such as the MWCM. In case of the latter, the prediction ratio takes the form

$$p = \frac{\Delta\tau_{N,i}}{\Delta\tau_{Rm,N,i}} \qquad (26)$$

where the $\Delta\tau_{N,i}$ is the shear stress range on the critical plane and $\Delta\tau_{Rm,N,i}$ is the modified shear stress resistance at the same number of cycles, N, calculated using the associated modified slope $m_{m,i}$ of the i'th specimen.

The prediction ratio is calculated for each specimen using the different criteria and plotted in histograms in Figure 10. A 3 parameter Weibull distribution is fitted to each data set in order to calculate the probability of non-conservative predictions, $P_{NC}[\%]$, i.e. the probability of a test results falling below the SN curve.

The resulting probabilities of non-conservative prediction are listed in Table 2 for each of the multiaxial criteria.

Table 2: Probability of non-conservative prediction P_{NC} for each multiaxial criteria when evaluated against FAT225/3 and FAT160/5.

Criterion	Loading	
	Proportional	Non-proportional
Principal stress	13.6%	45.6%
von Mises	12.8%	27.1%
Eurocode 3	10.8%	20.4%
IIW recommendations	14.9%	3.6%
Sonsino EESH	8.6%	0.1%
Carpinteri-Spagnoli	13.9%	27.9%
Findley	5.4%	17.8%
Susmel MWCM	10.7%	36.7%

Referring to Figure 10a, the plot shows the prediction ratio for the reference data, i.e. the bending/tension only specimens evaluated using the normal stress range $\Delta\sigma_x$ against the FAT225/3 SN curve. Similarly Figure 10b shows the torsion/shear only specimens evaluated using the shear stress range $\Delta\tau_{xy}$ against the FAT160/5 SN curve, respectively. For these two cases, the probability of non-conservative prediction is $P_{NC} = 4.5\%$ and 1.7%, respectively.

Although these values cannot be directly compared with SN curve probability of failure ($P_f = 5\%$ in the IIW system [7]) they are in the expected order of magnitude.

The remaining plots in Figure 10 (c to j) shows the prediction ratio calculated using the 8 multiaxial criteria for the specimens under combined loading. These
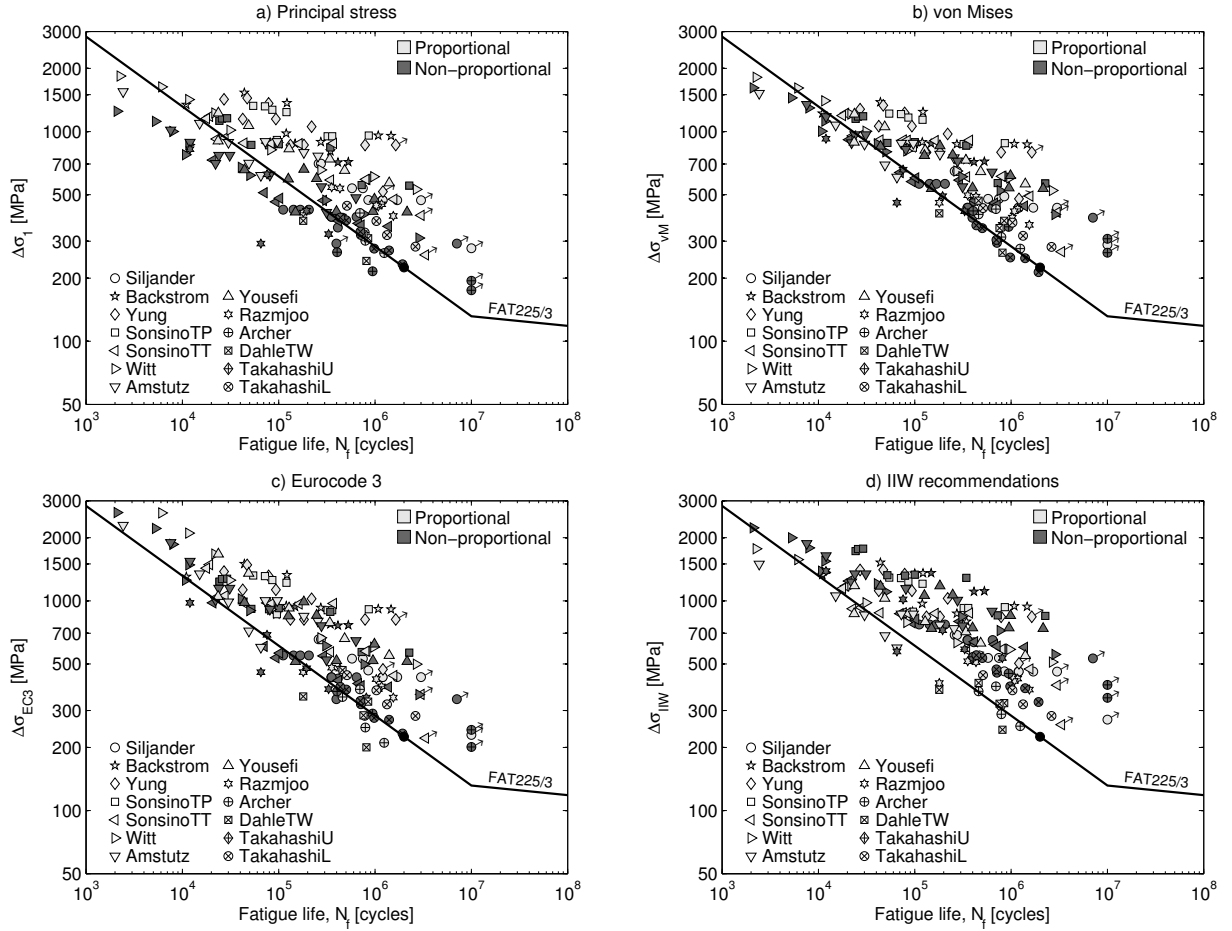
Figure 8: Evaluation of equivalent stress and interaction equations.

plots show the same data as in the SN diagrams in Figures 8 and 9. The light gray bars and curves represent proportional loading, whereas the darker ones represent non-proportional loading. Atop each histogram the median ± 1 standard deviation is shown for the prediction ratio.

Most criteria show the best performance under proportional loading, with probabilities of non-conservative predictions generally in the range of 9 − 15%, except the Findley criteria, which achieves the best results with $P_{NC} = 5.4\%$

All criteria, except the IIW and the EESH, shows higher probability of non-conservative prediction under non-proportional loading compared to proportional loading. Several other comments must be made regarding these two criteria. They are by far the most safe with

$P_{NC} = 0.1 − 3.6\%$ but at the same time the most scattering and at times over conservative. E.g. approximately half the predictions of the EESH have $p \geq 2$. Likewise, they are the only ones in which the calculation of the equivalent stress range deviates between proportional and non-proportional loading. Considering this, it is thus not surprising that these criteria achieves the safest results for non-proportional loading.

The principal stress approach on the other hand (Figure 8a and 10c), shows the most troubling finding of this study, i.e. 45.5% non-conservative predictions in case of non-proportional loading. For proportional loading, the approach is on par with most other criteria. The IIW recommendation of not using this approach for non-proportionally loading should thus be taken very seriously.
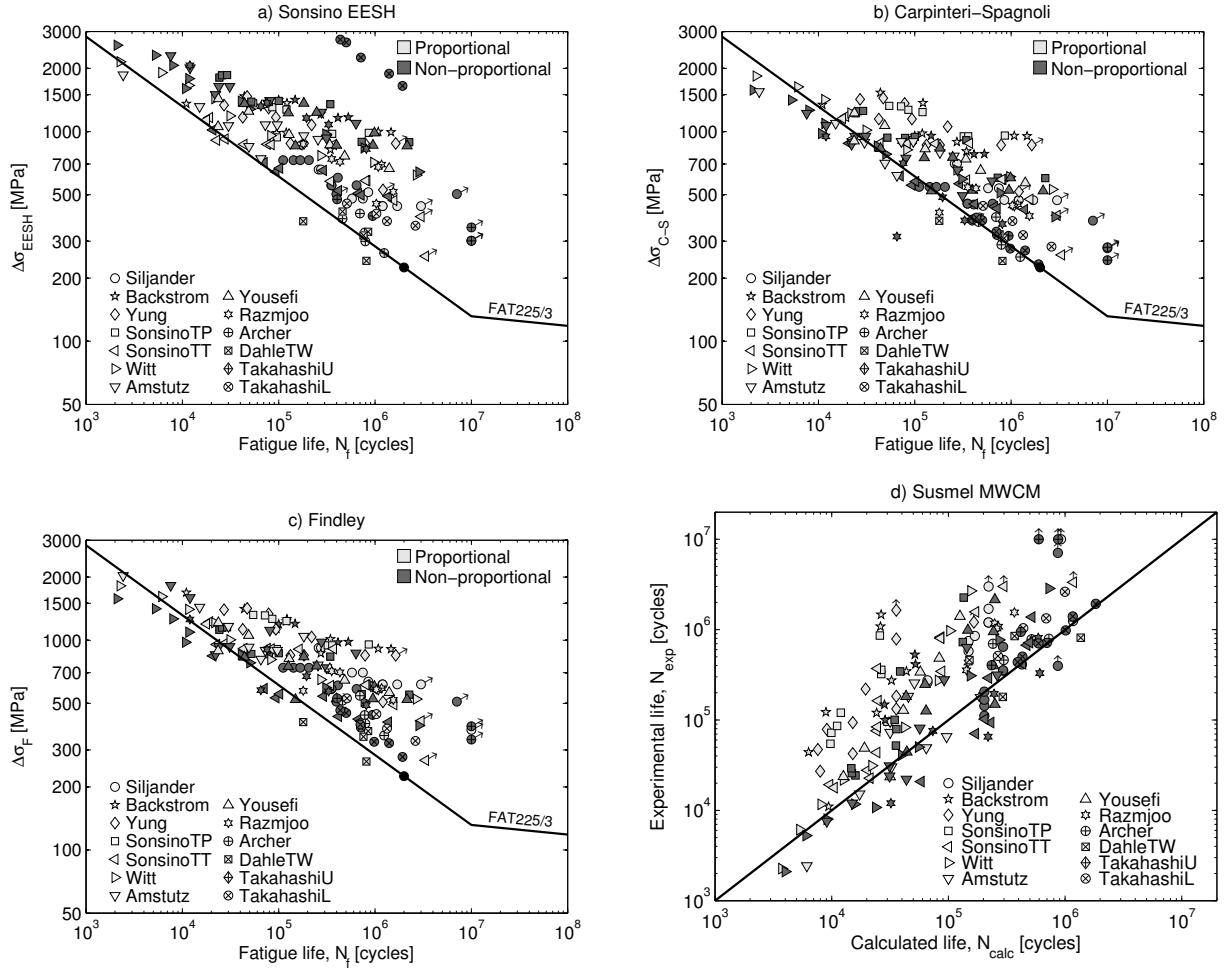
9

Figure 9: Evaluation of critical plane approaches.

Using the von Mises equivalent stress, Figure 8b and 10d, covers the data somewhat better, both regarding proportional and non-proportional loading.

Comparing the EC3 and IIW interaction equations (Figure 8a and b and 10e and f), it is seen that the IIW approach is superior for non-proportional loading. The performance under proportional loading, on the other hand is more even. The IIW correction for non-proportional loading (using a lower $CV = 0.5$) corresponding to a penalty factor of $1/\sqrt{0.5} = 1.41$ on the stress range is relatively crude, but it does provide almost exclusively safe results ($P_{NC} = 3.6\%$).

The EESH, Figure 9a, generally provides the most safe results overall, maybe a bit on the conservative side

for non-proportional loading, Figure 10g. A drawback of this approach is that it needs very specific information (e.g. $K_{t,\tau}$ and δ) which is available for fatigue tests, but may be unknown in practice, i.e. the stress concentration factor may be difficult to determine in case of complex geometry (due to ill-defined nominal stress) and the phase shift between the loading may vary. Also in the case of non-torsional secondary loading, e.g. Takahashi [26], the shear stress concentration factor $K_{t,\tau}$ becomes very small and the assessment thus very conservative.

For proportional loading, the Carpinteri-Spagnoli criteria corresponds to the principal stress approach with the addition of a mean stress correction (eq. (19)), but since most test results are obtained under $R = -1$, the

effect is minor. For non-proportional loading, on the other hand, the shear stress range is included in the calculation of the effective stress range scaled by a factor of $k = 1.98$ according to eq. (18).

From the analysis of the MWCM results, it turns out that the limit value on the modified slope $m_m \geq m_\sigma$ is crucial for the performance, whereas the limit on the stress ratio ρ_w seems less significant. Considering non-proportional loading, the MWCM is the second least safe of the criteria with $P_{NC} = 36.7\%$. It does however show the least amount of scatter in the prediction results, Figure 10j. For proportional loading, the results are on line with the other criteria.

The two reference SN curves (FAT225/3 and FAT160/5) should not be blamed for the poor performance of some the criteria, since they both cover the uniaxial test results very well.

More conservative assessments could of course be obtained using the rotated SN curves proposed by Sonsino [18] ($m_\sigma = 5$ and $m_\tau = 7$) for thin or flexible specimens. However, considering the specimen geometries in Figure 5, none of them appear particularly thin or flexible in the opinion of the author, though this is of course a subjective judgment.

5. Conclusions

This paper presented a re-analysis of a large amount of fatigue test results of welded joints subjected to multiaxial loading. The investigation is carried out using the notch stress approach and 8 different multiaxial criteria.

A quantitative evaluation is performed by calculating a prediction ratio for each test result using each of the multiaxial criteria. The population of prediction ratios is then subjected to statistical analysis and the probability of non-conservative prediction is determined for each criteria.

Here, it should be kept in mind that some of the scatter observed in the results may stem from other issues than just the multiaxial criteria, however the results presented here reflects the safety obtained in an engineering context when using the approaches described.

The following conclusions are drawn

1. The uniaxial reference SN curves FAT225/3 and FAT160/5 agree well with the experimental results studied here for pure bending/tension and torsion/shear, respectively.
2. The probability of non-conservative prediction is generally very high for non-proportional loading, up to 45%.

3. For proportional loading, the probability of non-conservative prediction is generally much lower, but still up to 15%.
4. The Findley criterion lead to the safest predictions for proportional loading.
5. The EESH and IIW criteria are recommended for non-proportional loading, since these showed the lowest probability of non-conservative predictions.

6. References

[1] S. J. Maddox, G. R. Razmjoo, Interim fatigue design recommendations for fillet welded joints under complex loading, Fatigue and Fracture of Engineering Materials and Structures 24 (5).

[2] W. Fricke, Guideline for the fatigue assessment by notch stress analysis for welded structures, IIW-Doc. XIII-2240r1-08.

[3] M. Bäckström, Multiaxial fatigue life assessment of welds based on nominal and hot spot stresses, Ph.D. thesis, Laapeenranta University, Finland (2003).

[4] O. A. Siljander, P. Kurath, F. V. Lawrence, Nonproportional biaxial fatigue of welded joints, UILU-ENG no. 158, University of Illinois (1991).

[5] C. M. Sonsino, Multiaxial fatigue assessment of welded joints - recommendations for design codes, Int. Journal of Fatigue 31 (2009) 173–187.

[6] Eurocode 3, Eurocode 3, Design of Steel Structures Part 1-9: Fatigue, CEN, 2005.

[7] A. Hobbacher, IIW Recommendations for Fatigue Design of Welded Joints and Components, Revised September 2013., IIW-doc. XIII-2460-13, 2013.

[8] J. Lemaitre, J.-L. Chaboche, Mechanics of solid materials, Cambridge University Press, 1994.

[9] C. M. Sonsino, Multiaxial fatigue of welded joints under in-phase and out-of-phase local strains and stresses, Int. Journal of Fatigue 17 (1) (1995) 55–70.

[10] C. M. Sonsino, T. Lagoda, Assessment of multiaxial fatigue behaviour of welded joints under combined bending and torsion by application of a fictitious notch radius, Int. Journal of Fatigue 26 (2004) 265–279.

[11] A. Carpinteri, A. Spagnoli, S. Vantadori, Multiaxial fatigue life estimation in welded joints using the critical plane approach, Int. Journal of Fatigue 31 (2009) 188–196.

[12] W. Findley, A theory for the effect of mean stress on fatigue of metals under combined torsion and axial load or bending, Journal of Engineering for Industry (1959) 301–306.

[13] G. Marquis, M. Bäckström, A. Siljander, Multiaxial fatigue damage parameters for welded joints: Design code and critical plane approaches, in: Proc. First North European Engineering and Science Conference, 1997.

[14] A. Bolchoun, C. Sonsino, H. Kaufmann, T. Melz, Multiaxial random fatigue of magnesium laserbeam-welded joints - experimental results and numerical fatigue life evaluation, Procedia Engineering 101 (2015) 61–68.

[15] O. Bruun, G. Härkegård, A comparative study of design code criteria for prediction of the fatigue limit under in-phase and out-of-phase tensiontorsion cycles, Int. Journal of Fatigue 73 (2015) 116.

[16] L. Susmel, Multiaxial Notch Fatigue, Woodhead Publishing, Cambridge, UK, 2009.

[17] L. Susmel, Four stress analysis strategies to use the Modified Wöhler Curve Method to perform the fatigue assessment of weldments subjected to constant and variable amplitude multiaxial fatigue loading, Int. Journal of Fatigue 67 (2014) 38–54.

[18] C. M. Sonsino, T. Bruder, J. Baumgartner, SN-curves for welded thin joints - suggested slopes and FAT-values for applying the notch stress concept, IIW doc. XIII-2280-09.

[19] J.-Y. Yung, F. V. Lawrence, Predicting the fatigue life of welded joints under combined bending and torsion, in: M. W. Brown, K. J. Miller (Eds.), Biaxial and multiaxial fatigue, EGF3, Mechanical Engineering Publications, London, 1989, pp. 53–69.

[20] M. Witt, H. Zenner, Multiaxial fatigue behaviour of welded flange-tube connections under combined loading. experiments and lifetime calculation., in: 5th International Conference on Biaxial/Multiaxial Fatigue and Fracture, Cracow, Poland, 1997, pp. 421–434.

[21] H. Amstutz, K. Störzel, T. Seeger, Fatigue crack growth of a welded tubeflange connection under bending and torsional loading, Fatigue and Fracture of Engineering Materials and Structures 24 (2001) 357–368.

[22] F. Yousefi, M. Witt, H. Zenner, Fatigue strength of welded joints under multiaxial loading: experiments and calculations, Fatigue and Fracture of Engineering Materials and Structures 24 (5) (2001) 339355.

[23] G. R. Razmjoo, Fatigue of load-carrying fillet welded joints under multiaxial loading, in: Fatigue - Core research from TWI, European Structural Integrity Society, Vol. 22, Woodhead Publishing, 2000, p. 153164.

[24] R. Archer, Fatigue of a welded steel attachment under combined direct stress and shear stress, in: International conference of fatigue of welded constructions, no. paper 50, TWI, Brighton, England, 1987.

[25] T. Dahle, K. E. Olsson, B. Jonsson, High strength welded box beams subjected to torsion and bending - test results and proposed design criteria for torsion/bending interaction, in: Proc. First North European Engineering and Science Conference, Stockholm, Sweden, 1997, pp. 143–161.

[26] I. Takahashi, A. Takada, M. Ushijima, S. Akiyama, Fatigue behaviour of box-welded joint under biaxial cyclic loading: effects of biaxial load range ratio and cyclic compressive loads in the lateral direction, Fatigue and Fracture of Engineering Materials and Structures 26 (2003) 439–448.

[27] C. M. Sonsino, Suggested FAT classes for the notch approach design of welded joints according to the notch stress concept with the reference radius r = 1.00 and 0.05mm, IIW doc. XIII-2216-08.

[28] B. Jonsson, Z. Barsoum, A. G. Bazou, Influence from weld position on fillet weld quality, IIW doc. XIII-2273-09.
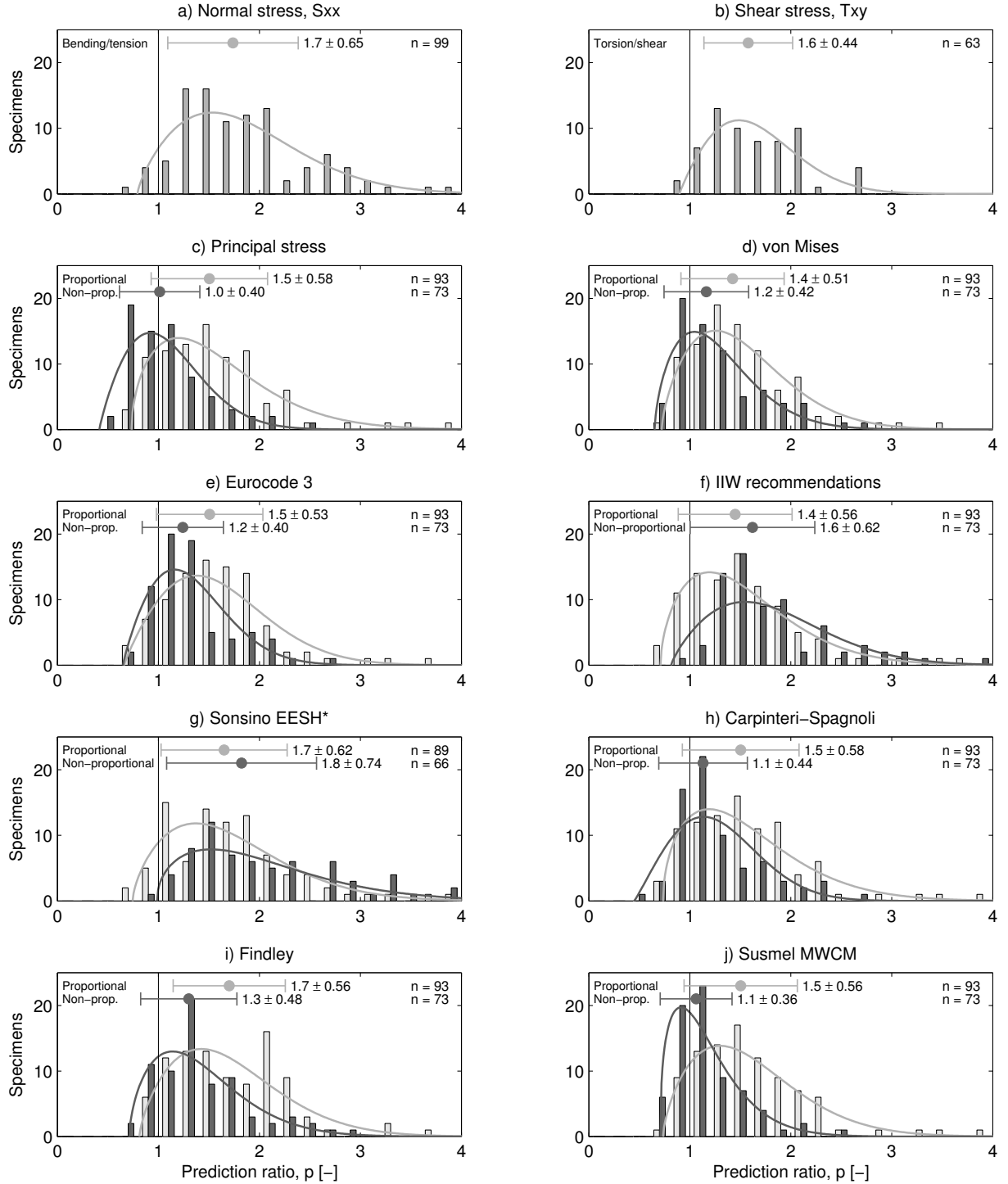
Appendix A. Tables

Figure 10: Distribution of the prediction ratio for the uniaxial reference data and each multiaxial criteria. *TakahashiL results excluded.

Table A.3: Fatigue test series data. [1]Count used here. [2]Typical value (varies). [3]Torsion specimens machined, corrected by 1/1.3 [4]Secondary load not shear, but transverse tension (σ_y)

Author	No.[1]	R_σ	R_τ	τ/σ	Material	Stress relieved	Dimensions [mm]
Siljander [4]	38	-1;0	-1;0	0.42[2]	ASTM A519	yes	∅50.8x9.5
Bäckström [3]	22	-1;0;> 0	-1;0	0.43[2]	S355	no	SHS100x100x5
Yung [19]	18	-1	-1	0.58[2]	ASTM A519	some	∅47.6x8
Sonsino (TP) [9]	34	-1	-1	0.58	StE460	yes	∅88.9x10
Sonsino (TT) [9][3]	46	-1	-1	0.58	StE460	yes	∅88.9x6
Witt [20]	41	-1;0	-1;0	1.00	S460M	yes	∅84.9x8
Amstutz [21]	37	-1;0	-1;0	1.00	StE460	yes	∅88.9x10
Yousefi [22]	40	-1	-1	1.00	P460	yes	∅84.9x8
Razmjoo [23]	28	0	0	> 1.00[2]	BS4360-50D	no	∅48.6x3.2
Archer [24]	22	0	-1	1.00	BS4360-43C/A	no	Beam 192x200x8
Dahle [25]	8	-1	-1	≈ 1.00[2]	Domex 350	no	Beam 150x150x10
Takahashi [26][4]	17	0	0;< −1	≈ 1.00[2]	JIS SM400B	no	100x12 longitudinal

Table A.4: Notch stress at unity nominal stress.

Author	Type	Primary load						Type	Secondary load					
		σ_x	σ_y	σ_z	τ_{xy}	τ_{yz}	τ_{xz}		σ_x	σ_y	σ_z	τ_{xy}	τ_{yz}	τ_{xz}
Siljander	Bending	2.34	0.76	0.15	0.00	-0.00	-0.53	Torsion	0.00	-0.00	-0.00	1.63	-0.33	0.00
Backstrom	Bending	3.45	1.07	0.75	0.06	-0.01	-0.81	Torsion	0.00	-0.01	-0.00	1.42	-0.39	0.00
Yung	Bending	2.80	0.96	0.25	-0.00	0.00	-0.65	Torsion	-0.00	-0.00	-0.00	1.57	-0.35	0.00
SonsinoTP	Bending	3.31	1.14	0.16	-0.00	0.00	-0.68	Torsion	-0.00	-0.00	-0.00	1.74	-0.34	-0.00
SonsinoTT	Bending	1.65	0.22	0.04	0.01	0.01	-0.22	Torsion	-0.00	0.02	-0.02	1.36	-0.17	0.07
Witt	Bending	2.88	1.04	0.24	-0.00	-0.00	-0.61	Torsion	-0.00	0.00	-0.00	1.62	-0.33	-0.00
Amstutz	Bending	3.31	1.14	0.16	-0.00	0.00	-0.68	Torsion	-0.00	-0.00	-0.00	1.74	-0.34	-0.00
Yousefi	Bending	2.88	1.04	0.24	-0.00	-0.00	-0.61	Torsion	-0.00	0.00	-0.00	1.62	-0.33	-0.00
Razmjoo	Tension	4.06	1.85	0.19	-0.00	-0.00	-0.83	Torsion	0.00	0.00	0.00	1.46	-0.29	0.00
Archer	Bending	2.00	0.40	0.11	-0.01	0.00	-0.42	Shear	0.07	-0.02	0.00	1.57	-0.33	-0.01
DahleTW	Bending	1.79	0.30	0.14	-0.00	-0.00	-0.43	Torsion	0.00	-0.00	0.00	1.55	-0.39	-0.00
TakahashiL	Tension	2.62	0.43	0.38	0.04	-0.01	-0.67	Tension	-0.84	0.39	-0.13	-0.01	0.00	0.23
TakahashiU	Tension	3.15	0.62	0.41	0.05	-0.01	-0.76	None	-	-	-	-	-	-

Table A.5: Nomenclature

σ_x	normal stress perpendicular to weld	θ	search plane rotation angle
σ_y	normal stress parallel to weld	ϕ	search plane inclination angle
τ_{xy}	shear stress parallel to weld	ρ_w	critical plane stress ratio
$\Delta\sigma_1$	principal stress range	m_m	slope of modified SN curve (MWCM)
$\Delta\sigma_{vM}$	von Mises stress range	$\Delta\tau_{Rm}$	fatigue strength of modified SN curve (MWCM)
$\Delta\sigma_{EC3}$	EC3 equivalent stress range	f	Findley damage parameter
$\Delta\sigma_{IIW}$	IIW equivalent stress range	f_{crit}	critical value of the Findley parameter
$\Delta\sigma_R$	normal stress fatigue strength	σ_{max}	maximum normal stress over cycle
$\Delta\tau_R$	shear stress fatigue strength	$F(\theta)$	EESH damage parameter
D	damage	$\Delta\sigma_{EESH}$	EESH equivalent stress range
CV	comparison value	f_s	EESH size factor
$\boldsymbol{\sigma}$	stress tensor	N	number of cycles
$\mathbf{S_n}$	stress vector on plane	$\Delta\sigma_n$	normal stress range on critical plane
$\boldsymbol{\sigma_n}$	normal stress on plane	$\Delta\sigma_{C-S}$	Carpinteri-Spagnoli stress range
$\boldsymbol{\tau}$	shear stress on plane	$\Delta\sigma_{eq}$	equivalent normal stress range
$\mathbf{n}$	plane unit normal vector	σ_m	mean stress
P_f	probability of failure	P_s	probability of survival
m	slope of SN curve	R	stress ratio
m_σ	slope of normal stress SN curve	m_τ	slope of shear stress SN curve
t	plate thickness [mm]	$K_{t,\sigma}$	stress concentration factor (normal stress)
μ	Poisson's ratio	$K_{t,\tau}$	stress concentration factor (shear stress)
k_m	correction for misalignment	Rm	tensile strength [MPa]
k	constant	δ	phase shift in loading
p	prediction ratio	P_{NC}	probability of non-conservative prediction